Studying the high frequency seismic signals for enhanced knowledge of the shallow Earth structure and soil investigation

Mohamed A. GAMAL ⬥, George MAHER* ⬥

Geophysics Department, Faculty of Science, Cairo University, Giza, Egypt
e-mails: magamal@sci.cu.edu.eg, georgemaher55@yahoo.com

Abstract: The Earth acts like a low-pass filter to earthquake energy so that frequencies higher than 10 Hz are rapidly attenuated. This intrigues seismologists about the seismic waves in the frequency domain $1-10$ Hz, which is crucial to correctly assess the impact of seismic shaking on structures. However, not much attention has been paid to higher frequencies, probably due to its low significance and structural damage. The Earth has high frequency seismic signal (HFSS) in the audible frequency range $20-20,000$ Hz and maybe higher (*Gamal et al., 2020*). These seismic signals result from the transformation of any energy into HFSS energy which is propagated inside the Earth, this energy may be winds, the crustal structure movement, movement due to gravitational force or any mechanical energy transformed into high frequency seismic vibrations. Fifteen different geological environments were tested in Egypt, to monitor the high frequency seismic signals (HFSS) of the subsurface soil. The present study used very high digitising frequency seismographs, not less than 8,000 to 16,000 sample per second, and a set of horizontal and vertical geophones of natural frequencies in the ranges of 4 Hz to 100 Hz. It was found that consolidated rocks have high-pitch that may reach 4,000 Hz, while weak fractured soils sound have a low-pitch, in the frequency range of $20-70$ Hz. Speech and audio processing methods have been used to differentiate between these HFSS preserved inside soils and to produce the "unified HFSS map". The "Soil HFSS map" was considered as avail science could be used in the future to give deep insight on the shallow Earth's interiors.

Key words: high frequency, seismic signal, seismic waves, sound waves, spectrograms, voice recognition, soil recognition

1. Introduction

Early studies showed that noises emanating from Earth's interior are of low amplitudes, microns in the frequency range $1-10$ Hz and they were called

---

*corresponding author, e-mail: mgeorge@sci.cu.edu.eg

"microtremors". *Kanai (1957)* became the first scientist to introduce the concept of using microtremors to determine the soil's natural frequency of vibration which can evaluate the soil's interaction with earthquake energy. Several subsequent studies were conducted to determine the "soil response" to the earthquake energy and its effects on buildings (*Aki, 1957; Kanai and Tanaka, 1961; Kanai, 1962; Nogoshi and Igarashi, 1970; Kagami et al., 1982 & 1986; Rogers et al., 1984; Çelebi et al., 1987; Lermo et al., 1988; ECP, 1993; Nakamura, 1989, 1997 & 2000; Bour et al., 1998; Diagourtas et al., 2002; Gamal, 2009; Harutoonian et al., 2012; Mahajan et al., 2012; Hunstad et al., 2013; Adib et al., 2015; Akkaya, 2015; Ridwan et al., 2014; Jiang et al., 2016; Singh et al., 2017; Gamal et al., 2019 & 2020, Gamal and Maher, 2022*).

Mucciarelli (1998) excluded some surface sources such as winds or sounds from sources such as winds entering the asphalt layers, making asphaltic waves. *Mucciarelli (1998)* considered it as a bad source that may led to bad determination of soil responses. *Nakamura (1989)* used the little excitation for the soil or the so-called microtremors to study the dynamic properties of the site, such as period and amplitude. Such old studies were mainly based on "low frequency energy", inaudible to human ears $(1-20\,\mathrm{Hz})$. Such studies were succeeded to explicate the interaction between the soil response and the earthquake energy and its effects on buildings (*Horike, 1985; Field et al., 1990; Ishida et al., 1998; Miyakoshi et al., 1998; Scherbaum et al., 1999; Yamamoto, 2000*).

There are three identifiable types of waves: seismic waves, sound waves and ultrasound waves (Fig. 1; Table 1). The human ear could recognise frequencies in the range of 20 Hz to 20 kHz (Fig. 1, *Pilhofer and Day, 2007*). Seismic waves are generated from the mechanical vibrations produced from seismic sources such as explosions or earthquakes. Such low-frequency waves, far from their sources, in the range of $1-20\,\mathrm{Hz}$ are too low to be heard by humans.

Table 1. Main difference between seismic waves and sound waves (*Dobrin, 1952*).

Wave Type	Period (Sec)	Frequency (Hz)	Wavelength
Seismic waves (Body waves)	$0.01-50$	$0.02-100$	$50\,\mathrm{m}-500\,\mathrm{km}$
Seismic Waves (Surface waves)	$10-350$	$0.003-0.1$	$30\,\mathrm{km}-1{,}000\,\mathrm{km}$
Sound Waves	$0.05-0.00005$	$20-20{,}000$	$17\,\mathrm{mm}-17\,\mathrm{m}$
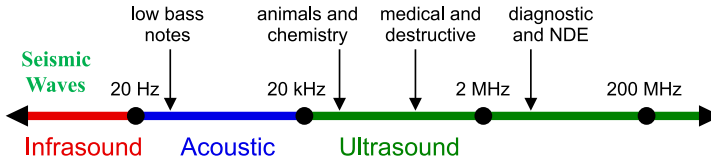
Fig. 1. Comparison between infrasound (1 – 20 Hz, not audible to the human ear), acoustic waves (20 Hz – 20 kHz, audible to the human ear) and the ultrasound waves (20 kHz – 200 kHz, above human hearing ability, *Pilhofer and Day, 2007; Hunstad et al., 2013* and *Levitin, 1999*).

Every animal being on Earth has its own auditory and phonation apparatus that enables them to produce a unique sound wave. Sounds differ according to the variations in the auditory and phonation apparatus, such as the vocal cord length, size, type and dimensions of the throat cavity. These differences leaded to product a sound waves various in some items such as; sound pitches, energy entering each pitch, and the unique spaces between these pitches or formants. Soil is like animal beings each spot has its own "high frequency seismic signal", but this is different from normal speech, however, it has unique sound pitches.

2. Spectrograms

Spectrograms provide a standard, powerful technique for analysing the frequency content of sound recordings as well as seismograms. For instance, *Chen et al. (2013)* showed the discrepancy between landquakes, local and teleseismic earthquakes (Fig. 2). The spectrogram of local earthquake shows seismic energy of a much wider frequency content showing a sudden appearance after the first arrival time, followed by an exponential decay (*Chen et al., 2013*). The spectrograms were calculated by the S-transformation (*Stockwell et al., 1996*).

Burtin et al. (2014) also studied the frequencies of waves which resulted from cross rock volumes. Figure 3 shows spectrograms of a rockslide recorded in the Illgraben catchment in the Swiss Alps. These spectrograms display the emergence of seismic energy at high frequencies, and highlights activity of two different sources. The first one was related to the slope failure and lasted for about 10 s, while the second one reflected the rolling and tumbling of rock debris down the slope over a period of about 1 min.
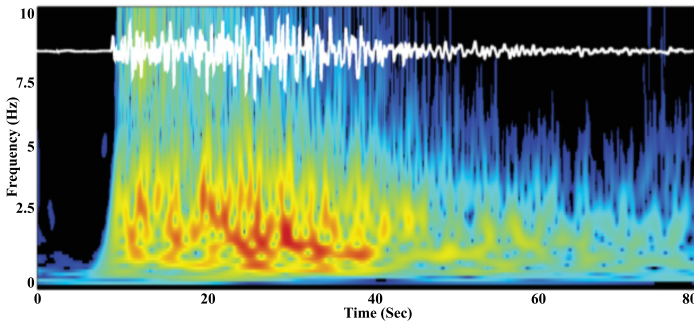
Fig. 2. Spectrogram of local earthquake. White traces are the original vertical-component velocity record (*Chen et al., 2013*).
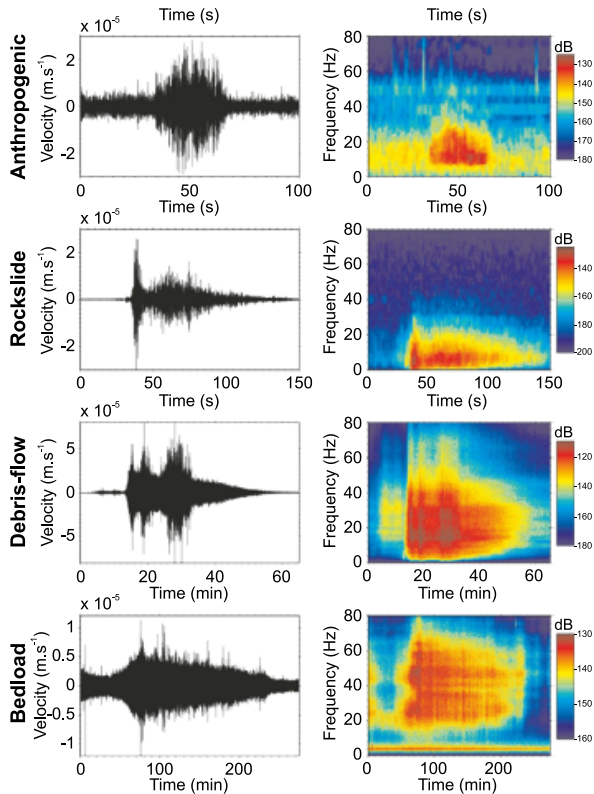
Fig. 3. Characterization of seismic signals (left) with a time-frequency analysis (right). From top to bottom Anthropogenic activities, a rockslide (Illgraben, day 1/2013), a debris-flow and bedload transport (*Burtin et al., 2014*).

4

3. Methodology and data processing

Different geophones were used in the current study including the P-wave geophones with frequency of 4 Hz, Triaxial 4 Hz geophone and Downhole triaxial geophone (4 Hz). In each site, external unwanted sources of noises or sounds in case of recording calm soil conditions were removed carefully. To get HFSS, the recorded signals were maintained small as 0.5 or 2 s in order to get high samples ranging between 8,000 – 16,000 samples, for each record. More than 20 records were taken at each site to show the true effect of each soil station at each site. For quality control over the data, lots of stations were distributed at each site with different conditions including calm, noisy, remote areas, areas surrounded by buildings etc. The geophones were buried to get rid of wind noises as possible and only firm soil conditions were used with good coupling with geophones.

3.1. Data processing

The main processing steps applied to the "seismic signals" are the following:

– Conversion of signal from seg2 format into standard Ascii formats;

– Merged all collected data into one segment signal;

– View signals in time domain and removed the unwanted HFSS peaks if necessary (such as sudden strikes);

– To produce soil calm conditions the unwanted sources of HFSS which affect the natural soil resonance pitches were removed (Hammers, falling objects, HFSS of nearby cars, airplanes or any moving objects);

– Making programs or codes capable of producing high quality "seismic signal spectrogram" with full control over the parameters used to calculate it such as:

    i. Capability of changing the size of the window's used to calculate the "HFSS spectrogram";

    ii. Capability of changing the size of the overlap window;

    iii. Capability of changing the method used to calculate the spectrogram (e.g. Rectwin, Gauss or Blackman etc.);

– Comparing different directions spectrograms like vertical or horizontal channels;

- Full control over colour, time, frequency and possibility to cut bad parts and save the best data;
- Clean Data were then transformed into spectrograms with window size 8,000 samples or 3,000 samples;
- Overlap between samples is 70% or more depending on the quality of the produced spectrogram;
- Type of spectrogram used (Blackman, Gauss, rectwin etc.) are acting like the lens of a camera that may give very clear pictures or bad pictures, Hence the program was used and the parameters were fixed for all data.

Recently, we set up a script that calculates the spectrograms and make it audible by playing these HFSS and see them at the same time. All the parameters used to introduce these spectrograms are listed in *Gamal and Maher (2022)*. Figure 4 is the first audible/visible sample of Earth soil collected at Ras Gharib site in Egypt. To get spectrograms of high precision, we fully controlled the parameters used to calculate the spectrograms especially since this was the first time we would see and listen to the "High frequency seismic signal preserved inside Earth".
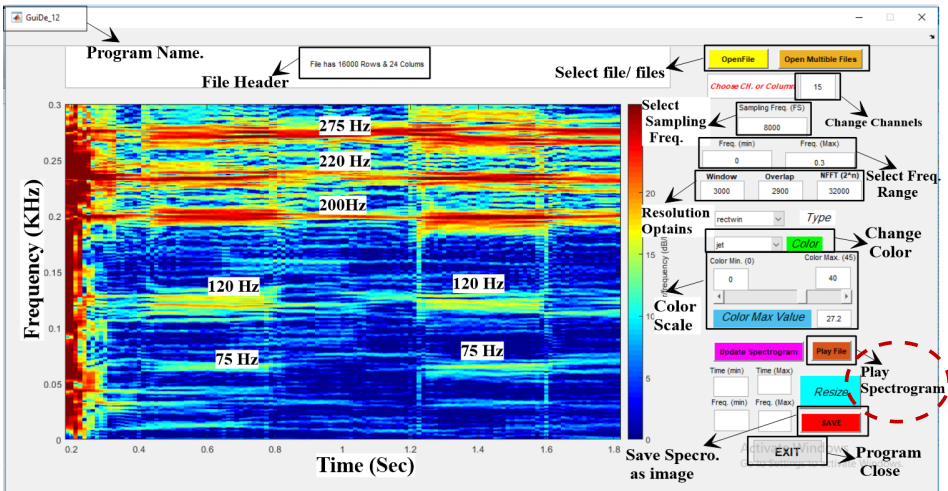
Fig. 4. SpectroPro4 software was used to produce high resolution audible/visible spectrograms to show HFSS signals from Earth using MATLAB R2018a code. The software could control different parameters to calculate the spectrograms and play its sound (*Gamal and Maher, 2022*).

Figure 5 displays the audible/visible sample of Earth soil "High frequency signals" collected at the 6th of October City, Giza governorate, Egypt showing the following features:

– Resonance peaks for times 10 Hz, 25 Hz, 38 Hz, 50 Hz, and 70 Hz;

– Variation in the amount of energy, for example, energy is high and wide at the low seismic range between 1–10 Hz, while it is high but tight and sharper in the audible range 38 Hz, 50 Hz and 70 Hz;

– Variation in the amount of energy at pitch 25 Hz is relatively low energy compared with the other pitches. This is most probably due to the change in the source of the energy;

– Like atom energy levels, each Earth soil signal has energy levels prepared to acquire the HFSS energy in the resonance pitch domains. This is expected to be the nature of each unique place on Earth. These domains are preserved to acquire HFSS energy and are thought to be a nature of sites rather than sources;

– Most importantly, the spectrogram can be played these HFSS samples to see and hear what these Earth soil "high frequency signal" like to be able to identify the differences and explore Earth's interiors.

Table 2, showed the relative strength of some soils in Egypt at which the spectrograms were calculated) based on the SPT refusal depth value
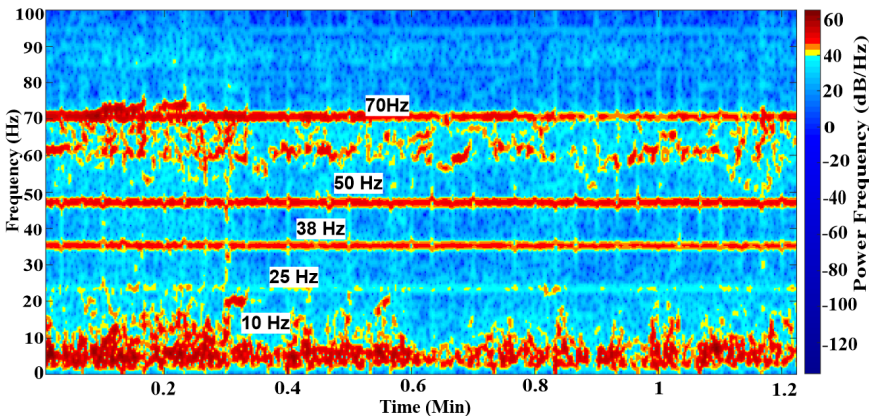
Fig. 5. The first visible/audible Earth soil "High frequency signal" sample recorded from 6th of October City's soil, showing soil resonance pitches or formants at 10 Hz, 25 Hz, 38 Hz, 50 Hz, and 70 Hz. Note the variation in the amount of energy with time.

(standard penetration test) N30 ≥ 50, which is defined as the depth at which 50 blows in sandy soil is not enough to make the spoon penetrates 30 cm.

Table 2. Comparison between relative soil strength derived from SPT test refusal depth (N30 ≥ 50) and maximum pitch frequency obtained in this study.

Soil name	Main soil composition	Maximum "resonance pitch" obtained by soil (Hz)	SPT soil refusal depth (m)	Relative strength
Port Said	Soft Clay	8	20	Very Weak
El-Waraq soil	Soft Clay	25	25	Weak/Saturated
Ain El-Sokhna	Sand/Crushed L.S.	40	6	Medium
6th of October	Silty Sand	70	8	Medium
Ismailia	Sand	250	7	Medium
Abu Rudies	Sand/Coral L.S.	265	5	Medium to Strong
Ras Gharib	Vugy Sandstone/ Sand and Silt	275	6	Medium to Strong
New Giza	Thick Limestone	2,900	–	Very Strong

4. Exploring Earth's interiors by listening to Earth soil "high frequency signal" in Egypt

Earth soil "High frequency signal" collected in this study are ranging from 10 Hz to < 4,000 Hz in frequency/ pitch. We were able to collect 15 samples in Egypt, which could be considered an appropriate environment for capturing different types of "high frequency seismic signals" as it has various geological environments such as soft soils composed of sand (6th of October City), soft clays (Port Said City, El Waraq Island) and hard rocks (New Giza City or Abu Rudies City, Fig. 8). To obtain high resolution visible/audible spectrograms of the soil "high frequency seismic signals", the samples were collected using the following instruments and parameters:

– A highly digitised seismograph capable of recording 8,000 – 16,000 samples per second;

– P-wave geophones with frequency 4 Hz, Triaxial 4 Hz geophone and 4 Hz Downhole triaxial geophone were used (14 Hz S-wave geophones, 40 Hz

p-wave geophones and 100 Hz p-wave geophones were also tested but not generalized);

– The record length of signal is ranged between 0.5 to 30 s. But when signal is weak we extended it into several minutes. Almost in most cases, the recorded files were kept small to keep the sampling high (8,000 – 16,000 SPS) in order to get minimum 4,000 Hz frequency spectrograms.

Figure 6 displays the spectrogram of El-Waraq island site, which is composed of alluvium deposits giving three main resonance pitches 3 Hz, 15 Hz and 25 Hz. This soil is considered as a relatively weak composed of soft clay saturated by water which is located at the canter of the River Nile (*Azer et al, 2016*). While the spectrogram of Ain El-Sokhna site is giving resonance
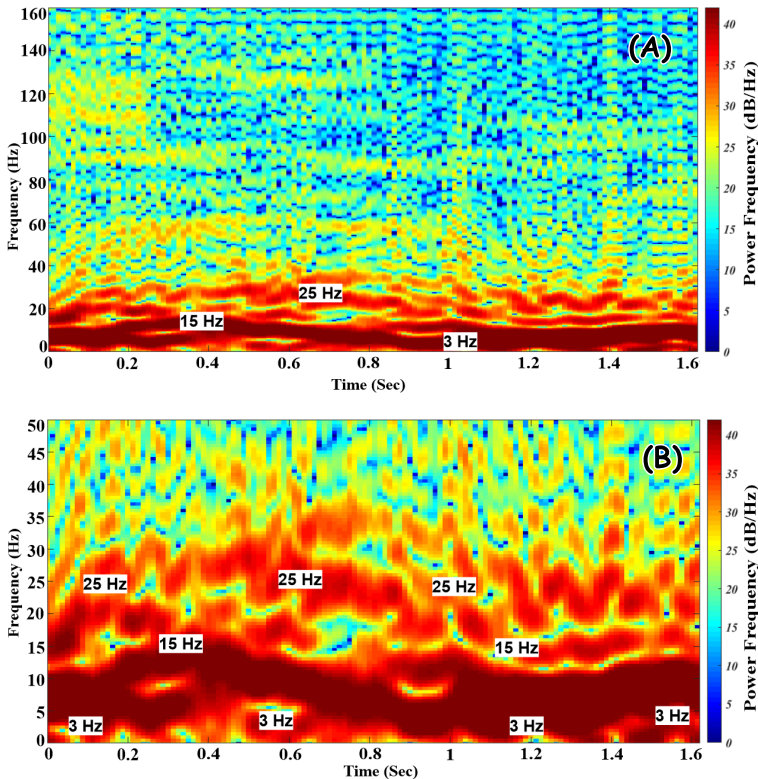
Fig. 6. Spectrogram calculated for EL-Waraq island site shows the resonance pitches at 3 Hz, and 15 Hz, these pitch frequencies are inaudible to the human's ear. Note: Figure (B) is zooming of Figure (A).

9

pitches at 10 Hz and 40 Hz (Fig. 7), it is composed of compacted sand and crushed limestone and is showing relatively medium strength (Table 2).
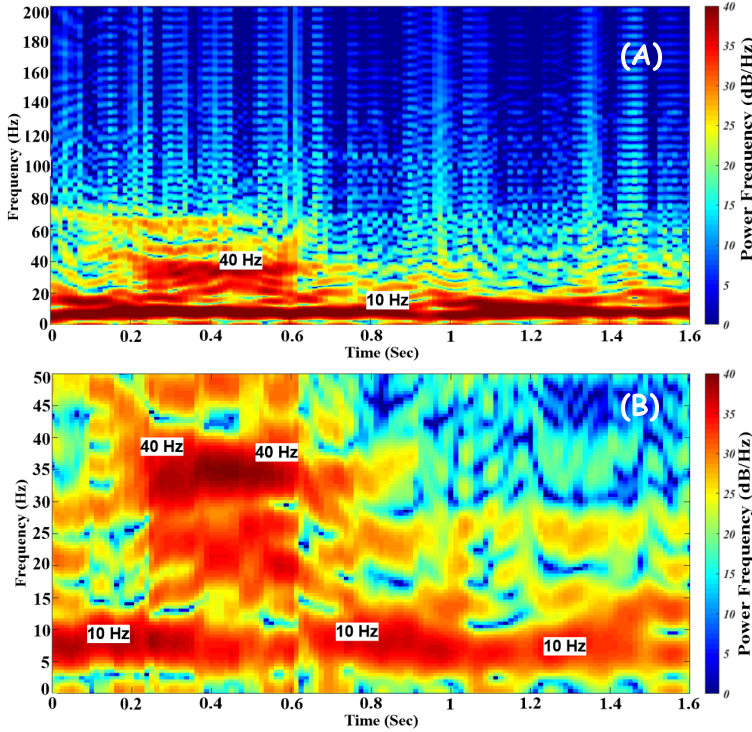
Fig. 7. Spectrogram calculated from Ain El-Sokhna site showing the resonance pitches at 10 Hz, and 40 Hz. Note: Figure (B) is zooming of Figure (A).

5. From voice recognition into soil recognition

5.1. Excluding HFSS properties the way the human ear does

Since HFSS are simpler in recognition than human speech, voice recognition and speaker identification methods were used for soil recognition. The method was applied for fifteen soil samples collected in different geological conditions (Fig. 8, *Singh et al., 2012*). The human ear is sensitive to lower frequencies that travel further along to reach the nerves rather than the high frequencies that vibrate at the entrance of the ear. For this reason, almost all filters designed to simulate the ear are closely spaced in the beginning

and sparsely toward the end (Fig. 9). The filterbank used in the current study to exclude the HFSS properties is shown in Fig. 9.
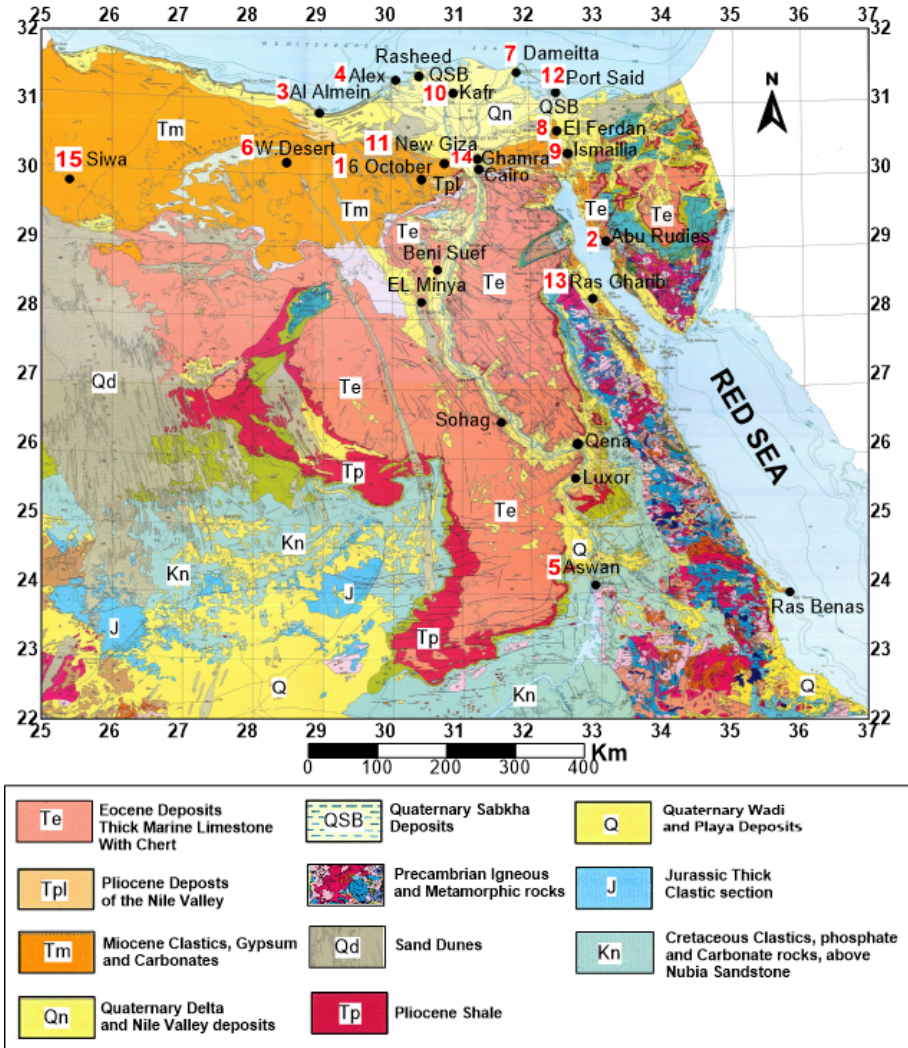
Fig. 8. A simplified geological map of Egypt showing the locations of the 15 sites of Earth soil HFSS signals in different geological environments (*EGS, 1981*, http://www.egsma.gov.eg). [1] 6th of October City, [2] Abu Rudies, [3] Al Almein, [4] Alexanderis, [5] Aswan. [6] The Western Desert, [7] Damietta, [8] EL Ferdan, [9] Ismailia, [10] Kafr El Sheikh, [11] New Giza, [12] Port Said, [13] Ras Gharib, [14] Ghamra and [15] Siwa.
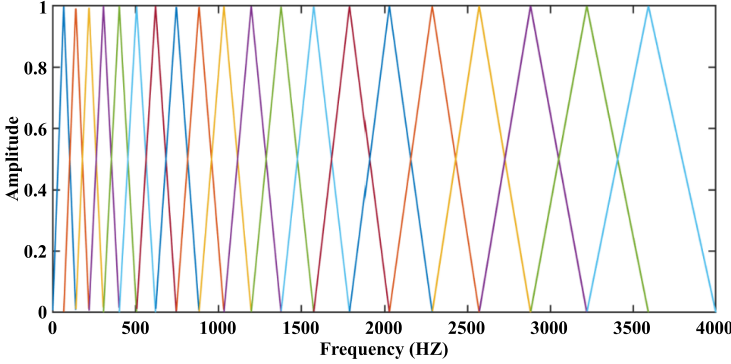
Fig. 9. Filterbank or triangular filters which used to compute the mel-cepstrum in this study (Eq. (2)).

5.2. Excluding Earth soil HFSS properties using mel-frequency cepstral coefficient features

The word "cepstral" is the inverse of the word spectrum and is used to determine sound properties by excluding the so-called mel-frequency cepstral coffiecients (MFCC) (*Gaikwad et al., 2010*), as described briefly in the following steps.

Davis and Mermelstein (1980) presented the MFCC feature extraction in the subsequent steps:

Given the DFT of the input signal:

$$X_a[k] = \sum_{n=0}^{N-1} x[n]\, \mathrm{e}^{\frac{-j2\pi nk}{N}}, \qquad 0 \le k < N. \tag{1}$$

We can define filter bank with M filters ($m = 1, 2, \dots M$), where filter m is triangular filter given by the following equation:

$$H_m[k] = \begin{cases} 0 & k < f[m-1] \\[2mm] \dfrac{2(k - f[m-1])}{(f[m+1] - f[m-1])(f[m] - f[m-1])} & f[m-1] \le k \le f[m] \\[2mm] \dfrac{2(f[m+1] - k)}{(f[m+1] - f[m-1])(f[m+1] - f[m])} & f[m] \le k \le f[m+1] \\[2mm] 0 & k > f[m+1]. \end{cases} \tag{2}$$

12

Such filters compute the average spectrum around each centre frequency with increasing Bandwidths, and they are displayed in Fig. 9.

F_s: is the sampling frequency ($8,000 - 16,000$ SPS in this study);

f_1: lowest frequency (1 Hz) in filterbank;

f_h: highest frequency (4,000 Hz) in filterbank;

M: the number of filters (head of the triangles Fig. 9);

N: the size of the FFT.

The boundary points $f[m]$ are uniformly spaced in the mel-scale as follows:

$$f[m] = \left(\frac{N}{F_s}\right) B^{-1}\left(B\left(f_1\right) + m\frac{B\left(f_h\right) - B\left(f_1\right)}{M+1}\right), \tag{3}$$

where B is mel-scale frequency analysis used in modern speech recognition and is given by:

$$B[f] = 1125 \ln\left(1 + \frac{f}{700}\right). \tag{4}$$

B^{-1} is its inverse and is given by:

$$B^{-1}[b] = 700 \left(e^{\left(\frac{b}{1125}\right)} - 1\right). \tag{5}$$

The Mel frequency cepstral coefficients $C[n]$ are calculated using the discrete cosine transform of the M filter outputs, where n is the number of coefficients which is taken as 26 coefficients in this study (Fig. S1, in supplement).

$$C[n] = \sum_{m=0}^{M-1} S[m] \cos\left(\frac{\pi n \left(m + \frac{1}{2}\right)}{M}\right), \qquad 0 \leq n < M. \tag{6}$$

Upon plotting the MFCC curves, it can be considered as the voice prints for different speakers or different Earth soil HFSS signals. As can be seen in Fig. S1 (in supplement), the MFCC sound properties and curves for a mother and her son are close in shape, while they are different in a stranger's voice. The same phenomenon occurred upon comparing two Earth soil HFSS signals collected from different parts of Earth, as shown from the samples taken in Abu Rudies City and Ras Gharib City, which are 60 km apart (Fig. S2, in supplement).

5.3. 2D humans and Earth voice prints

The excluded MFCCs for each human voice or Earth soil HFSS can be used to identify or differentiate between varying voices by drawing these data as vectors and calculating their centroids. The centroids of the data could be calculated using the vector quantisation k-means algorithm (*Lloyd, 1982; Seber, 1984; Späth, 1985; Arthur and Vassilvitskii, 2007*). The k-means method is a technique used to seek and minimise the average squared distance between points in the same cluster. This distance is a property of sound and can be used to identify or differentiate between voices. For example, the soil HFSS collected from nearby sites show similar clustering of MFCC vectors data. Also, the centroids calculated using the k-means method for the three soil HFSS samples collected at 6th of October City are nearly the same (Fig. S3, in supplement). These centroids can be considered HFSS voice prints, and since the soil HFSS collected in 6th of October City are spaced by about 5 metres, the three soil HFSS' centroid locations and data trends are identical (Fig. S3, in supplement). This could be attributed to the similarity in soil composition for the three collected samples. However, when the distance between soil HFSS' locations are bigger, the soil composition varies, leaving different vectors and centroids, as seen in New Giza and Port Said's soil HFSS (Fig. S4, in supplement).

Most studies on speaker identification uses both MFCC and vector quantisation methods to differentiate between voices by plotting the MFCC data to find the centre of the data for each speaker using the vector quantisation method (Fig. S5, in supplement, *He et al., 1999; Huang et al., 2001; Young et al., 2006; Dhingra et al., 2013; Thakur and Sahayam, 2013; Nijhawan and Soni, 2014; Sunitha and Chandra, 2015*). Vector quantisation was used to separate a large data vector into small regions. Each region consists of clusters for each speaker data and can be represented by its centre or centroid (*Hasan et al., 2004*). The collection of the entire speaker signal was called a codebook and was used to differentiate between speakers.

5.4. The unrepeatable voice prints

Earth soil HFSS can be used to make like voice prints for some important features such as water and oil or even native elements such as gold or diamond. Most MFCC/vector quantisation methods use only two MFCCs

such as MFCC1 and MFCC2, two dimension (2-D) plots to differentiate between HFSS. However, using two MFCC was not enough to obtain a unique voiceprints for soil, using the complete HFSS properties such as 25 MFCC's can lead to more accurate, appropriate, and unrepeatable HFSS properties. To achieve this, we used machine learning or the so-called t-SNE method (*Jacobs, 1988; Van der Matten and Hinton, 2008*), which stands for t-distributed Stochastic Neighbor Embedding algorithm and was used to reduce the multidimensional data, visualising it in 2D or 3D (*Van der Matten and Hinton, 2008*). While the t-SNE method makes compact multidimensional data, it uses all of the dimensions to get unique final 2D results that simplify and use all the dimensions. Therefore, it was more accurate as it uses sound properties directly excluded from the sound. To show the efficiency of this method, we applied it to pure tones. Two similar records, each one two-seconds long, for the same pure tone C4 of a violin were used (Fig. S6, in supplement). The 25 MFCC features were excluded for both tones. As can be seen, the two similar pure tones are nearly the same using 25 MFCC sound properties or 25D of data (Fig. S7, in supplement).

This could be completely different if we compared two different pure violin tones such as C4 and C7 (Fig. S8, in supplement). To show the efficiency of t-SNE method in separating sounds, we compared almost all the low and sharp audible pitches for the C pure tones (C0 to C8) of the violin (Fig. S9, in supplement). The result was satisfactory: each tone made a unique geometrical shape at a specific domain separated from other tones (Fig. S9, in supplement). These unique geometrical shapes and specific locations are considered as voice prints in 25D for C pure tones (Fig. S9, in supplement).

Since Earth soil HFSS are composed of a superposition of pure tones, the same method was employed to compare different Earth soil HFSS signals. We started by comparing Earth soil HFSS from the same place before moving to other places. 21 Earth soil HFSS signals were collected in the same location at Ras Gharib City (Site-13, Fig. 8). The site was composed of Quaternary Wadi deposits underlain by igneous and metamorphic rocks and can be considered as medium to strong strength site (Table 2). The geophones were aligned and separated by 5 m. The excluded 25 MFCC sound properties and t-SNE method showed that all these soil HFSS make a unique geometrical shape and fit the same place, as can be seen in Fig. S10, in supplement.

To generalize this method, 15 more Earth soil HFSS were collected from all over Egypt's different geological environments and were plotted in one map (Fig. S11, in supplement). The map was introduced again using 25 MFCC HFSS properties and t-SNE method, showing different geological environments and HFSS properties. When Earth's elements share similarities such as in Kafr-El-Sheikh and Ismailia (soil composed mainly of sand), they interfere in some place (Fig. S11, in supplement). However, when HFSS properties are near and similar in soil composition, if the similarity was bigger, the soil HFSS may coincide with each other such as the soil of Siwa and Al Alamein which are made of saturated sand. We, therefore, introduced an "Earth HFSS Voice Print Map", which can differentiate between soils based on the signals emitted from it (Fig. S11, in supplement). For unknown HFSS, we can expect its composition using the world voice print map for all Earth elements.

6. Conclusion

Fifteen Earth soil "High frequency seismic signals" (HFSS) were collected from different geological environments in Egypt. The properties excluded from these soil HFSS signals are the so-called mel-frequency cepstral coefficients (MFCC). 25 MFCCs and t-SNE multi-reduction dimension methods were used to introduce the unique Earth HFSS voice prints in 25 dimensions. It was found that just like pure tones of a violin, similar places produce similar soil HFSS that have certain geometrical shapes and take specific domains. When these soil HFSS signals interfered in some areas, the properties of the soil were found to be similar in some parts. In this study, seismological stations capable of collecting 16,000 samples per second were used with variable frequency geophones ($4-100$ Hz) and a special software to calculate the spectrograms of soils. Weak soft soils were found to give low-pitched HFSS such as the soft clay soil of El-Waraq site (25 Hz), while hard rocks tend to give high-pitched HFSS such as the massive thick rocks of limestone from New Giza (3,500 Hz).

15 soil HFSS samples were collected in different geological environment in Egypt to produce Earth Voice Print Map for "high frequency seismic signal". When the sites were identical such as samples taken at Ras Gharib the soil HFSS were identical. But when sites were different the soil HFSS

took different shapes and locations. This is most probably due to change in lithology, compaction and chemical composition. On the other hand, when some soil properties are similar such as Kafr-El-Sheikh and Ismailia (both soils composed of mainly sand), the HFSS interfere. Some soil HFSS were found similar although they are far from each other's such as the soil of Siwa and Al Alamein. This was most probably due to similar geological compositions (which are made of saturated sand). The current study is important because transforming Earth's properties into sounds could be used to distinguish geological hazards such as land sliding zones and cavernous rocks. It could be used also in the future to distinguish between thousands of HFSS such as the HFSS of water-bearing or oil-bearing formations. It is expected that the soil recognition and speaker identification methods can be used in the future to know more about Earth's interior.

References

Adib A., Afzal P., Heydarzadeh K., 2015: Site effect classification based on microtremor data analysis using a concentration–area fractal model. Nonlinear Process. Geophys., **22**, 1, 53–63, doi: 10.5194/npg-22-53-2015.

Aki K., 1957: Space and time spectra of stationary waves, with special reference to microtremors. Bull. Earthq. Res. Inst. Univ. Tokyo, **35**, 3, 415–456.

Akkaya İ., Özvan A., Tapan M., Şengül M. A., 2015: Determining the site effects of 23 October 2011 earthquake (Van province, Turkey) on the rural areas using HVSR microtremor method. J. Earth Syst. Sci., **124**, 7, 1429–1443, doi: 10.1007/s12040-015-0626-1.

Arthur D., Vassilvitskii S., 2007: K-means++: The Advantages of Careful Seeding. SODA '07: Proceedings of the Eighteenth Annual ACM-SIAM Symposium on Discrete Algorithms, New Orleans, LA, January 7–9, 2007, 1027–1035.

Azer S. A., Fawzi N. M., Abdelmaksoud H. S., 2016: A study on the flora of Waraq Island at Giza governorate, Egypt. Egypt. J. Biotechnol., **53**, 53–71.

Bharti R., Bansal P., 2015: Real Time Speaker Recognition System using MFCC and Vector Quantization Technique. Int. J. Comput. Appl., 117, 1, 25–31, doi: 10.5120/20520-2361.

Bour M., Fouissac D., Dominique P., Martin C., 1998: On the use of microtremor recordings in seismic microzonation. Soil Dyn. Earthq. Eng., **17**, 7-8, 465–474, doi: 10.1016/S0267-7261(98)00014-1.

Burtin A.; Hovius, N.; Turowski J. M., 2014: Seismic monitoring of geomorphic processes. Earth Surf. Dyn. Discuss., **2**, 1217–1267, `doi: 10.5194/esurfd-2-1217-2014`.

Çelebi M., Dietel C., Prince J., Onate M., Chavez G., 1987: Site amplification in Mexico City (determined from 19 September 1985 strong-motion records and from records of weak motions). In: Cakmak A. S. (Ed.): Ground Motion and Engineering Seismology, Developments in Geotechnical Engineering book series, **44**, 141–152, Amsterdam, Elsevier, `doi: 10.1016/B978-0-444-98956-7.50013-1`.

Chen C.-H., Chao W.-A., Wu Y.-M., Zhao L., Chen Y.-G., Ho W.-Y., Lin T.-L., Kuo K.-H., Chang J.-M., C., 2013: A seismological study of landquakes using a real-time broad-band seismic network. Geophys. J. Int., **194**, 2, `doi: 10.1093/gji/ggt121`.

Davis S., Mermelstein P., 1980: Comparison of parametric representations for mono-syllabic word recognition in continuously spoken sentences. IEEE Trans. Acoust. Speech Signal Process., **28**, 4, 357–366, `doi: 10.1109/TASSP.1980.1163420`.

Dhingra S. D., Nijhawan G., Pandit P., 2013: Isolated speech recognition using MFCC and DTW. Int. J. Adv. Res. Electr. Electron. Instrum. Eng., **2**, 8.

Diagourtas D., Tzanis A., Makropoulos K., 2001: Comparative study of microtremor analysis methods. Pure Appl. Geophys., **158**, 2463–2479, `doi: 10.1007/PL00001180`.

Dobrin, M., 1952: Introduction to geophysical prospecting. New York-London, McGraw-Hill, 435 p.

ECP (Egyptian Code of Practice), 1993: ECP-201: Egyptian code for calculating loads and forces in structural work and masonry. Housing and Building National Research Center, Ministry of Housing, Utilities and Urban Planning, Cairo.

Field E. H., Hough S. E., Jacob K. H., 1990: Using microtremors to assess potential earthquake site response: A case study in Flushing Meadows, New York City. Bull. Seismol. Soc. Am., **80**, 6, 1456–1480, `doi: 10.1785/BSSA08006A1456`.

Gaikwad S. K., Gawali B. W., Yannawar P. A., 2010: Review on speech recognition technique. Int. J. Comput. Appl., **10**, 3, 16–24, `doi: 10.5120/1462-1976`.

Gamal M. A., 2009: Using microtremors for microseismic zonation in Cairo's crowded, urban areas. J. Seismol., **13**, 1, 13–30, `doi: 10.1007/s10950-008-9113-3`.

Gamal M. A., Khalil M. H., Maher G., 2019: Using Microtremors to delineate subsurface structures in Port Said, North Eastern Egypt. Environment, International Technology and Science Publications (ITS), 3, 2, 11–26, `doi: 10.31058/j.envi.2019.32002`.

Gamal M. A., Khalil M. H., Maher G., 2020: Monitoring and studying audible sounds inside different types of soil and great expectations for its future applications. Pure Appl. Geophys., Springer Nature Switzerland AG, **177**, 11, 5397–5416, `doi: 10.1007/s00024-020-02583-0`.

Gamal M. A., Maher G., 2022: How to differentiate between various soil strength, using audio processing methods (1–1000 Hz). Egypt. J. Appl. Geophys., **1**.

GSE (Geological Survey of Egypt), 1981: Geologic Map of Egypt, scale 1:2000000. The Egyptian Geological Survey and Mining Authority.

Harutoonian P., Leo C. J., Doanh T., Castellaro S., Zou J. J., Liyanapathirana D. S., Wong H., Tokeshi K., 2012: Microtremor measurements of rolling compacted ground. Soil Dyn. Earthq. Eng., **41**, 23–31, `doi: 10.1016/j.soildyn.2012.05.006`.

Hasan R., Jamil M., Rabbani G., Rahan S., 2004: Speaker identification using MEL frequency cepstral coefficients. 3rd International conference on Electrical and computer Engineering ICECE 2004, 28-30 December 2004, Dhaka, Bangladesh.

He J., Liu L., Palm G. A., 1999: A discriminative training algorithm for VQ-based speaker identification. IEEE Trans. Speech Audio Process., 1999, **7**, 3, 353–356, doi: 10.1109/89.759047.

Horike M., 1985: Inversion of phase velocity of long-period microtremors to the S-wave-velocity structure down to the basement in urbanized areas. J. Phys. Earth, 33, 2, 59–96, doi: 10.4294/jpe1952.33.59.

Huang X., Acero A., Hon H.-W., 2001: Spoken Language Processing: A guide to theory, algorithm, and system development. Prentice Hall, Upper Saddle River, NJ, USA, 314–315.

Hunstad I., Marsili A., Casale P., Vallocchia M., Burrato P., 2013: Seismic waves and sound waves: From earthquakes to music. Seismol. Res. Lett., **84**, 3, 532–535, doi: 10.1785/0220120095.

Ishida H., Nozawa T., Niwa M., 1998: Estimation of deep surface structure based on phase velocities and spectral ratios of long period microtremors. In: Irikura K., Kudo K., Okada H., Satasini T. (Eds.): Proceedings of 2nd Int. Symp. on the Effects of Surface Geology on Seismic Motion, Yokohama, Japan, 1998, 2,697–704.

Jacobs R. A., 1988: Increased rates of convergence through learning rate adaptation. Neural Netw., **1**, 4, 295–307, doi: 10.1016/0893-6080(88)90003-2.

Jiang Y., Gao Y., Wu X., 2016: The nature frequency identification of tunnel lining based on the microtremor method. Undergr. Space, **1**, 2, 108–113, doi: 10.1016/j.undsp.2016.12.001.

Kagami H., Duke C. M., Liang G. C., Ohta Y., 1982: Observation of 1- to 5-second microtremors and their application to earthquake engineering. Part II. Evaluation of site effect upon seismic wave amplification due to extremely deep soil deposits. Bull. Seismol. Soc. Am., **72**, 3, 987–998, doi: 10.1785/BSSA0720030987.

Kagami H., Okada S., Shiono K., Oner M., Dravinski M., Mal A. K., 1986: Observation of 1- to 5-second microtremors and their application to earthquake engineering. Part III. A two-dimensional study of site effects in the San Fernando Valley. Bull. Seismol. Soc. Am., **76**, 6, 1801–1812, doi: 10.1785/BSSA0760061801.

Kamale H. E., Kawitkar R. S., 2013: Vector quantization approach for speaker recognition. Int. J. Comput. Technol. Electron. Eng. (IJCTEE), **3**, Special Issue, 110–114, In: Proceedings of E-NSPIRE, National Level Conference held at Pravara Rural Engineering College, Loni, Maharashtra, India, March–April 2013.

Kanai K., 1957: The requisite conditions for predominant vibration of ground. Bull. Earthq. Res. Inst. Univ. Tokyo, **35**, 3, 457–471, doi: 10.15083/0000033939.

Kanai K., 1962: On the spectrum of strong earthquake motions. Primeras J. Argentinas Ing. Antisismica, **24**, 1, 68–73.

Kanai K., Tanaka T., 1961: On Microtremors VIII. Bull. Earthq. Res. Inst. Univ. Tokyo, **39**, 1, 97–114.

Lermo J., Rodríguez M., Singh S. K., 1988: The Mexico Earthquake of September 19, 1985—Natural Period of Sites in the Valley of Mexico from Microtremor Measurements and Strong Motion Data. Earthq. Spectra, **4**, 4, 805–814, `doi: 10.1193/1.1585503`.

Levitin D. J., 1999: Memory for musical attributes (chapter 17). In: Cook P. R. (Ed.): Music, Cognition, and Computerized Sound: An Introduction to Psychoacoustics. Cambridge, Massachusetts, The MIT Press, 105–127, `doi: 10.7551/mitpress/4808.003.0019`.

Lloyd S. P., 1982: Least Squares Quantization in PCM. IEEE Trans. Inf. Theory, **28**, 2, 129–137, `doi: 10.1109/TIT.1982.1056489`.

Mahajan A. K., Mundepi A. K., Chauhan N., Jasrotia A. S., Rai N., Gachhayat T. K., 2012: Active seismic and passive microtremor HVSR for assessing site effects in Jammu City, NW Himalaya, India—A case study. J. Appl. Geophys., **77**, 51–62, `doi: 10.1016/j.jappgeo.2011.11.005`.

Miyakoshi K., Kagawa T., Kinoshita T., 1998: Estimation of geological structures under the Kobe area using the array recordings of microtremors. In: Irikura K. (Ed.): Proceedings of the 2nd Int. Symp. on the Effects of Surface Geology on Seismic Motion, Yokohama, Japan, 1-3 December 1998, Volume 3 Balkema, Rotterdam, Brookfield, 691–696.

Mucciarelli M., 1998: Reliability and applicability of Nakamura's technique using microtremors: An experimental approach. J. Earthq. Eng., **2**, 4, 625–638, `doi: 10.1080/13632469809350337`.

Nakamura Y., 1989: A method for dynamic characteristic estimation of subsurface using microtremor on the ground surface. Q. Rep. RTRI, **30**, 1, 25–33.

Nakamura Y., 1997: Seismic vulnerability indices for ground and structures using microtremor. World Congress on Railway Research, Florence, Italy, November 1997.

Nakamura Y., 2000: Clear identification of fundamental idea of Nakamura's technique and its applications. 12WCEE, 2000, 2656.

Nijhawan G., Soni M. K., 2014: Speaker recognition using MFCC and vector quantisation. Int. J. Recent Trends Eng. Technol., **11**, 1.

Nogoshi M., Igarashi T., 1970: On the propagation characteristics of microtremors. J. Seismol. Soc. Jpn, **23**, 4, 264–280, `doi: 10.4294/zisin1948.23.4_264`.

Pilhofer M., Day H., 2007: Music Theory for Dummies. Wiley, 360 p.

Ridwan M., Afnimar A., Widiyantoro S., Irsyam M., Yamanaka H., 2014: Estimation of S-wave velocity structures by using microtremor array measurements for subsurface modeling in Jakarta. J. Math. Fundam. Sci., **46**, 3, 313–327, `doi: 10.5614/j.math.fund.sci.2014.46.3.9`.

Rogers A. M., Borcherdt R. D., Covington P. A., Perkins D. M., 1984: A comparative ground response study near Los Angeles using recordings of Nevada nuclear tests and the 1971 San Fernando earthquake. Bull. Seismol. Soc. Am., **74**, 5, 1925–1949, `doi: 10.1785/BSSA0740051925`.

Scherbaum F., Riepl J., Bettig B., Ohrnberger M., Cornou C., Cotton F., Bard P. Y., 1999: Dense array measurements of ambient vibrations in the Grenoble basin to study local site effects. AGU Fall meeting, San Francisco, December1999.

Seber G. A. F., 1984: Multivariate Observations. Hoboken, NJ: John Wiley & Sons, Inc., 686 p.

Singh A. P., Parmar A., Chopra S., 2017: Microtremor study for evaluating the site response characteristics in the Surat City of western India. Nat. Hazards, **89**, 3, 1145–1166, `doi: 10.1007/s11069-017-3012-2`.

Singh N., Khan R. A., Shree R., 2012: MFCC and prosodic feature extraction techniques: A comparative study. Int. J. Comput. Appl., **54**, 1, 9–13, `doi: 10.5120/8529-2061`.

Späth H., 1985: Cluster Dissection and Analysis, theory, FORTRAN programs, examples. Translated by J. Goldschmidt. New York: Halsted Press, 226 p.

Stockwell R. G., Mansinha L., Lowe R. P., 1996: Localization of the complex spectrum: the S transform, IEEE Trans. Signal Process., **44**, 4, 998–1001, `doi: 10.1109/78.49 2555`.

Sunitha C., Chandra E., 2015: Speaker Recognition using MFCC and Improved Weighted Vector Quantization Algorithm 2015, Int. J. Eng. Technol. (IJET), ISSN 0975-4024, **7**, 5, 1685–1692.

Thakur A. S., Sahayam N., 2013: Speech Recognition Using Euclidean Distance Int. J. Emerg. Technol. Adv. Eng., **3**, 3, 587–590.

Van der Maaten L., Hinton G., 2008: Visualizing Data using t-SNE. J. Mach. Learn. Res., **9**, 2579–2605.

Yamamoto H., 2000: Estimation of shallow S-wave velocity structures from phase velocities of love and Rayleigh-waves in microtremors. In: Proceedings of 12th World Conf. on Earthquake Engineering, Auckland, New Zealand, 2000, paper No. 2239.

Young S., Evermann G., Gales M., Hain T., Kershaw D., Liu X., Moore G., Odell J., Ollason D., Povey D., Valtchev V., Woodland P., 2006: The HTK Book (for HTK Version 3.4). Cambridge University Press, 359 p.